International Journal of Business and Quality Research

https://e-journal.citakonsultindo.or.id/index.php/IJBQR
E-ISSN: 2985-9468

Recent Advances Of Pollutants Degradation In Different Environment By ZrO_2 Based Catalyst Activated Peroxymonosulfate

Hamza Khaliq[1], Faiza Shahzad[1], Arslan Riaz[2], Muhammad Mohsin[3], Rana Mohsin Ali[1,4*]

[1]College of Environment, Hohai University, Nanjing 210098, China
[2]School of Environmental Science and Engineering, Nanjing University, Nanjing 210023, China
[3]College of Chemistry, Xian Jiaotong University, Xian 710049, China
[4]School of Ecology and Environment, Zhengzhou University, Zhengzhou 450001, China

Corresponding Author: mohsincuf15@gmail.com

Abstract

Peroxymonosulfate (PMS) based advanced oxidation processes (AOPs) have drawn great attention as potential technology for abatement of the refractory organic pollutants in water and soil. Zirconium dioxide (ZrO_2) has garnered substantial research interest in the field of photocatalytic water treatment due to its appealing properties, such as thermal stability, considerable physical strength, and strong chemical resistance. Fe, Mn and a bimetallic Fe, Mn catalysts supported on ZrO_2 were synthesized and tested for the activation of persulfate (PS) and peroxymonosulfate (PMS) in the degradation reaction of three different organic compounds: cinnamic acid (CA), benzoic acid (BA), and catechol (C). The reversible conversion between ZrS_3 and ZrS_2 has been observed for the first time by thermal decomposition of ZrS_3 at 650 °C and sulfurization of ZrS_2 in sulfur vapor at 550 °C. This result suggests a potential application of ZrS_2 in the H_2S splitting process for H_2 recovery. Carbothermal reduction of Zr-sucrose gels powders into nano-phase ZrC, or ZrC-Zr (C,O) core-shell powders, via a composite of 2–4 nm sized ZrO_2 and amorphous carbon, is described. In future, various techniques have been utilized to enhance the efficiency of zirconium dioxide such as doping, metal loading. Although co-catalysts have gained a lot of interest by researchers, more efforts should be directed in strengthening the binding force between the co-catalyst and the semiconductor.

Copyright to the author of some rights reserved This work is licensed under aCreative Commons Attribution-ShareAlike 4.0 International License.

International Journal of Business and Quality Research
https://e-journal.citakonsultindo.or.id/index.php/IJBQR
E-ISSN: 2985-9468

Moreover, high cost of noble metals, aggregation and corrosion can be overcome by replacing the noble metals with cheap transition metals; thus more investigation is required in that field.

Keywords: Semiconductors, Zirconium dioxide, AOPs

INTRODUCTION

Peroxymonosulfate (PMS) based advanced oxidation processes (AOPs) have drawn great attention as potential technology for abatement of the refractory organic pollutants in water and soil. Among various methods for the activation of PMS, cobalt catalysis was found to be an efficient approach, in which the reactive sulfate radicals ($SO_4^{\cdot-}$) and hydroxyl radicals ($^{\cdot}OH$) were reckoned as the predominant reactive species (Siting Shao, 2022). Zirconium dioxide (ZrO_2) has garnered substantial research interest in the field of photocatalytic water treatment due to its appealing properties, such as thermal stability, considerable physical strength, and strong chemical resistance. However, the wide bandgap energy endorses less photo absorption and rapid charge carrier recombination kinetics, thus restricting the photoactivity of ZrO_2 (Rani, 2022). The three major polymorphs of ZrO_2, namely monoclinic, tetragonal, and cubic crystal structures are depicted in **Figure 1**. At ambient temperature, the monoclinic stage remains constant, but when heated to 1170 °C, it transforms to the tetragonal ZrO_2 and further to cubic ZrO_2 by increasing the temperature up to 2370 °C. The transformation is reversible when the temperature is lowered; the shift from tetragonal to monoclinic occurs at a lower temperature (around 950 °C) (Zhou, et al., 2019).

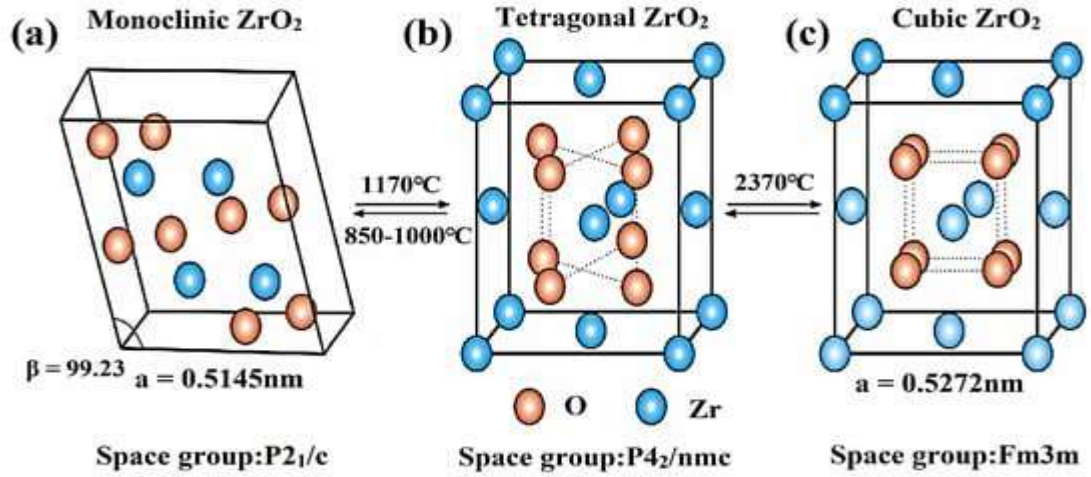


Fig. 1 Schematic representation of crystal structures of ZrO_2 (**a**) monoclinic ZrO_2, (**b**) tetragonal ZrO_2, and (**c**) cubic ZrO_2.

Copyright to the author of some rights reserved This work is licensed under aCreative Commons Attribution-ShareAlike 4.0 International License.

International Journal of Business and Quality Research
https://e-journal.citakonsultindo.or.id/index.php/IJBQR
E-ISSN: 2985-9468

Photocatalysis is an interesting AOP that has been given substantial attention due to its features like effective degradation of pollutants without generating harmful by-products, cost-effectiveness, high efficiency, and the ability to operate under the illumination of solar light (Pelosato, Bolognino, Fontana, & Sora, 2022). Recent research has manifested that zirconia-based materials show high redox abilities, large surface area, and low thermal conductivity in photocatalytic processes. In this regard, Aldeen et al. comprehensively explored the altered ZrO_2 based photocatalysts for organic pollutant degradation (Aldeen, et al., 2022). To overcome this, various enhancement strategies like doping, heterojunction formation incorporation of cocatalysts, etc., have been potentially explored. For instance, Co doped ZrO_2 synthesized by facile-chemical precipitation showed greater degrading activity against MB dye when exposed to visible light due to the improved dielectric properties (Ahmed & Iqbal, 2020). Zirconium dioxide (ZrO_2)-based semiconductors photocatalysts have recently gained much interest due to their outstanding effectiveness under visible irradiation for wastewater decontamination (Aziz et al., 2021). The graphene derivatives supported on ZrO_2 are mainly intriguing due to their unique electrical structures and outstanding photocatalytic performance (Shen et al., 2021; Gurushantha et al., 2017). Fe, Mn and a bimetallic Fe, Mn catalysts supported on ZrO_2 were synthesized and tested for the activation of persulfate (PS) and peroxymonosulfate (PMS) in the degradation reaction of three different organic compounds: cinnamic acid (CA), benzoic acid (BA), and catechol (C). The catalysts were prepared and tested in order to evaluate the effect of the metal and the metal combination on the generation of reactive oxygen species (ROS). The characterization of the catalysts was carried out by X-ray diffraction (XRD), X-ray photoelectron spectroscopy (XPS), and atomic absorption spectroscopy (AAS). The best degradation results were obtained when PMS was activated with the bimetallic Fe-Mn/ZrO_2 catalyst in the CA degradation. Moreover, the Fe-Mn/ZrO_2 catalyst reusability was tested for up to three consecutive cycles of reaction, with mineralization levels >90%. Mono- and bimetallic Fe-Mn catalysts supported on Z were prepared, with a total nominal metal content up to 4%wt. The obtained materials were named Fe_xMn_y, being x and y the nominal content of each metal in the catalyst. The employed synthesis for the preparation of the catalysts was previously reported by Garcia et al [28] In brief, NH_4OH (28% in NH_3) was added to a 0.4 M zirconium oxychloride solution, at room temperature, until pH 10. Zirconium hydroxide $Zr(OH)_4$ was then obtained as a pale yellow precipitate. Incipient wetness impregnation was employed for the Fe and/or Mn deposition. For that purpose, $Fe(NO_3)_3$ and $Mn(NO_3)_2$ aqueous solutions of the desired concentration were added to the zirconium hydroxide. The liquid to solid ratio was kept as 0.4 mL/g [29]. Finally, the solids were dried in air and kept at 383 K for 24 h. Then, they were calcined at 873 K in air for 4 h (Camila M. Loffredo, Fe-Mn/ZrO2

Copyright to the author of some rights reserved This work is licensed under aCreative Commons Attribution-ShareAlike 4.0 International License.

International Journal of Business and Quality Research
https://e-journal.citakonsultindo.or.id/index.php/IJBQR
E-ISSN: 2985-9468

catalysts: Sulfate-based-advanced oxidation process for the degradation of olive oil industry model pollutants, 2023).

Catalytic Activity of Fe-Mn/ZrO_2:

PMS was used as part of the triple salt commercially known as Oxone® ($KHSO_5$•½$KHSO_4$•½K_2SO_4), while PS was used in the form of its potassium salt ($K_2S_2O_8$). All the reactions were carried out in a glass batch reactor, containing 75 mL of a solution of 20 mg L^{-1} of CA, 50 mg L^{-1} of C, or 30 mg L^{-1} of C at 30 °C. The reactions were carried out without adjustment of pH. The solid oxidant (0.285 g of PMS or PS) and the catalyst (0.100 g) were added into the initial pollutant solution, under constant mechanical stirring. Suspension aliquots (3 mL) were withdrawn at predetermined intervals and filtered immediately through a Micropore membrane (pore size 0.45 µm). The UV–Visible spectra were collected (λ = 200–600 nm) in UV–Vis Cecil 2021 or UV–Vis Agilent Cary 60 spectrometers. The reactions were followed up to 240–270 min. The decrease in the main absorption bands of the contaminants, characteristics of the π → π * transition in aromatic compounds (λ_{max} BA = 228.0 nm at pH = 4.3; λ_{max} C = 275.5 nm at pH = 5; λ_{max} CA = 279.0 nm at pH = 4.7) was followed to evaluate the progress of the degradation reaction.

Control experiences were carried out to evaluate the degradation of the contaminants with the oxidizing agent in the absence of catalyst. In addition, the possible adsorption of the pollutants onto the catalyst surface was also analyzed. Moreover, the activity of the Z support without metal loading was evaluated in the degradation reactions. The consumption of the oxidant during the reaction was followed and determined using spectrophotometric methods [30,31], mainly based on the reactions of the remnant PS and PMS anions with I^- (Eq. 1 and Eq. 2). The colored complex that appears after the reaction has a strong absorption band with a maximum at 395 nm (reaction with PMS) and 352 nm (reaction with PS).

$$HSO_5^{-}{}_{(ac)} + 3I^{-}{}_{(ac)} \longrightarrow SO_4^{2-}{}_{(ac)} + I_3^{-}{}_{(ac)}$$

$$S_2O_8^{2-}{}_{(ac)} + 3I^{-}{}_{(ac)} \longrightarrow 2SO_4^{2-}{}_{(ac)} + I_3^{-}{}_{(ac)}$$

The Total Organic Carbon (TOC) remaining in the solutions was measured using a TOC-LCPH/NPC (Shimadzu) in order to evaluate de degree of mineralization of the phenolic contaminants. It was calculated according to the following relationship:

$$\%\text{of mineralization} = (TOC_0 - TOC_t / TOC_0) \times 100$$

where TOC_0 (mg L^{-1}) is the total organic carbon in the initial solution and TOC_t (mg L^{-1}) is the TOC concentration at the reaction time t.

Copyright to the author of some rights reserved This work is licensed under aCreative Commons Attribution-ShareAlike 4.0 International License.

International Journal of Business and Quality Research
https://e-journal.citakonsultindo.or.id/index.php/IJBQR
E-ISSN: 2985-9468

The pH of the initial solutions and the residual liquids after reaction was measured with a pH-meter Orion 250Aplus equipped with a pH electrode.
The stability of the catalysts was tested by AAS through the measurement of the leached metals in the remaining solution after 4 h of reaction.

Quenching experiments were performed in order to determine the main ROS responsible for the degradation of pollutants. For that purpose, the reactions were repeated as it was described before with the addition of either tertbutyl alcohol (TBA) or ethanol (EtOH). An adequate amount of each alcohol in the respective reactions was added into the reactor before the addition of the catalyst and the oxidant. The alcohol: oxidant molar ratio was 150:1.

Synthesis of Zirconium Oxide Nanoparticle by Sol-Gel Technique

Zirconium (II) oxide (zirconia) is a refractory and chemically inert metal oxide which exists in several phases depending on temperature. Monoclinic phase is stable below 1000°C, tetragonal phase exist above 1170°C and transform to cubic phase after 2370°C. The use of sol-gel method in producing zirconia has gain research interest (Jaenicke et al, 2008). The chemistry involved in sol-gel reaction can be expressed as :

$$M(OR)_n + xH_2O \rightarrow M(OR)_{n-x}(OH)_x + XROH$$
$$M\text{-}OH + HO\text{-}M \rightarrow M\text{-}O\text{-}M + HO_2$$
$$M\text{-}OR + HO\text{-}M \rightarrow M\text{-}O\text{-}M + ROH$$

Stefanic et al. have study the influence of processing parameters (pH value, type of anion and reaction temperature) on the properties of hydrous zirconia. They mix zirconium n-propoxide in isopropanol with aqueous solutions of different pH value and ion types. After that they calcined the sample at 400°C. They obtain tetragonal zirconia as the dominant phase after calcinations. Stocker & Baiker have prepared zirconia aerogel by sol-gel method using tetra-n-butoxy zirconium (IV) and acid catalysis. They vary the acid to alkoxide ratio and types of alcoholic solvent in the reaction. They found out that zirconia aerogel prepared with acid-to-alkoxide ratio of 0.95 and butanol have the largest BET surface area (205 $m^2 g^{-1}$). Beena et al. synthesized nanocrystalline zirconia using sol-gel and precipitation techniques (Štefanić et al, 2000). For sol-gel synthesis, they dilute zirconium oxide to 30wt% by adding propanol, and then hydrolyze with dropwise ammonia solution under continuous stirring until pH 10-10.5. For precipitation synthesis, they dissolved zirconium oxychloride in distilled water and then hydrolyzed with dropwise ammonia solution under continuous stirring until pH 10-10.5. The precipitates is then filtered and washed with distilled water to remove chlorine ions. Both sol-gel and precipitate samples are dried in oven as well as under

Copyright to the author of some rights reserved This work is licensed under aCreative Commons Attribution-ShareAlike 4.0 International License.

vacuum in rotavapor before calcined at different temperature (400-700°C). They found out that sol-gel synthesis showed the stabilization of tetragonal phase at higher temperature. The zirconia crystallite size is 13-28nm for sol- gel synthesis and 11-37nm for precipitation synthesis. Ward & Ko synthesis zirconium oxide by sol-gel preparation. Zirconium n-propoxide mix with nitric acid and n-propanol is mixed with another solution containing n-propanol and water with vigorous stirring. The resulting gel is aged for 2 hours in room temperature before dry in vacuum oven or supercritical drying with carbon dioxide. They found out that gel time increases with increasing amount of nitric acid added. With increasing gel time, the condensation reaction have slow down, hence creating larger surface area ($134 m^2 g^{-1}$) and pore volume ($0.37 cm^3 g^{-1}$) product . Heshmat pour and co-workers synthesized zirconia nanoparticle via sol-gel method using glucose and fructose as organic additives. Propanol is added to dilute zirconium n-propoxide to 30 wt%. Ammonia solution is added dropwise to pH 9-10. Glucose and Fructose mixture with 1:1 mass ration is added into the solution under vigorous stirring. The resulting gel is dried in oven(110°C) for 12 hours and then calcined at temperature ranging from 300-700°C. They produce zirconia nanoparticles with crystallite size between 10-30nm and the organic additive is further stabilized tetragonal phase at 700°C (Lim et al., 2013). Metal sulfides, particularly zirconium sulfides, have been successfully synthesized from elemental zirconium and sulfur by a so-called diffusion method. The method allows one to control the morphology and phases of zirconium sulfides via tuning the reaction temperature and sulfur vapor pressure. At 550 °C and 650 °C, ZrS3 nanobelts with a width from 90 to 160 nm and a thickness of about 26 ± 8 nm and 6 ± 2 μm in length were experimentally synthesized. Wider (from 90 to 743 nm) and longer (19.7 ± 3.4 μm) ZrS_3 nanobelts can be obtained by increasing the sulfur vapor pressure. Meanwhile, flake-like ZrS_2 particles were produced at 750 °C. Experimental observation revealed that the liquid–solid mechanism, in combination with sulfur intercalation, is likely a major mechanism that is responsible for the formation of ZrS_3 nanobelts. The reversible conversion between ZrS3 and ZrS2 has been observed for the first time by thermal decomposition of ZrS_3 at 650 °C and sulfurization of ZrS_2 in sulfur vapor at 550 °C. This result suggests a potential application of ZrS_2 in the H2S splitting process for H_2 recovery. (Dang et al., 2020). Carbothermal reduction of Zr-sucrose gels powders into nano-phase ZrC, or ZrC-Zr(C,O) core-shell powders, via a composite of 2–4 nm sized ZrO_2 and amorphous carbon, is described. Samples with 1.7–20 sucrose-carbon:Zr ratio gels heated to 1495 °C at 10 °Cmin−1, with 3 and 30 min hold time were studied in detail using; TG, XRD, SEM, TEM, STEM-EDX, and XPS with Ar+-ion etching. After 1495 °C, 3 min, the samples with 12-20C:Zr ratios yielded weakly agglomerated 30 to 40 nm sized ZrC particles, surrounded by a dense 5 nm thick shell of Zr(C,O). With 5C:Zr significant amounts of ZrO_2 was present after heating at 1495 °C for 3

Copyright to the author of some rights reserved This work is licensed under aCreative Commons Attribution-ShareAlike 4.0 International License.

International Journal of Business and Quality Research
https://e-journal.citakonsultindo.or.id/index.php/IJBQR
E-ISSN: 2985-9468

min, while after 30 min annealing, ZrC particles without residual amorphous carbon was obtained. Minor amounts of zirconia was found in most samples, which in similarity with the 5 nm Zr(C,O) shell, is believed to stem from post synthesis oxidation. (katea et al., 2021).

SYNTHESIS METHODS

Hydrothermal/solvothermal method

The hydrothermal/solvothermal strategy is a synthesis method for the preparation of the ZrO_2 photocatalyst, which involves a sealed vessel with water or any organic solvent as a reaction medium (Ma, et al., 2021). The crystallization of catalyst occurs at high temperatures and pressure maintained in the vessel. This method leads to the formation of powders with fine size or narrow size distribution with good chemical homogeneity and is dependent on some reaction parameters such as reaction time, pH value, temperature, solvent, etc. Surfactants also inhibit the growth of crystals by forming an ultrathin structure. Parveen et al. showed the pH dependence of hydrothermal reaction involving coupling of PPy with ZrO_2 photocatalyst (Parveen & Surumbarkuzhali, 2020). Typically, the ZrO_2/PPy composite was fabricated by maintaining the hydrothermal reaction condition (180 °C/24 h) with the adjustment of pH value. The individual PPy and ZrO_2 system showed the planer-structured PPy nanosheets with spherical ZrO_2 particles. TEM results also revealed the wrinkled lamer structure nanosheets of PPy and ZrO_2 samples (**Figure 5**a). Besides pH, the hydrothermal temperature also affects the morphology of the particles. As Rashid et al. prepared the ZrO_2 doped $ZnCo_2O_4$ nanocomposites by the hydrothermal process with sulfate as a precursor, ethylene glycol (EG) and water as solvents at 250 to 650 °C calcination temperature (Rashid, Barakat, Mohamed, & Ibrahim, 2014). The maximum increase in the surface area of ZrO_2-$ZnCo_2O_4$ was achieved at 350 °C calcined temperature. After calcination, the ZrO_2-$ZnCo_2O_4$ showed the presence of granular particles. Furthermore, the SEM results revealed the appearance of uniform-size nanoparticles of ZrO_2-$ZnCo_2O_4$ composites at higher temperatures (**Figure 5**b).

Copyright to the author of some rights reserved This work is licensed under aCreative Commons Attribution-ShareAlike 4.0 International License.

International Journal of Business and Quality Research
https://e-journal.citakonsultindo.or.id/index.php/IJBQR
E-ISSN: 2985-9468

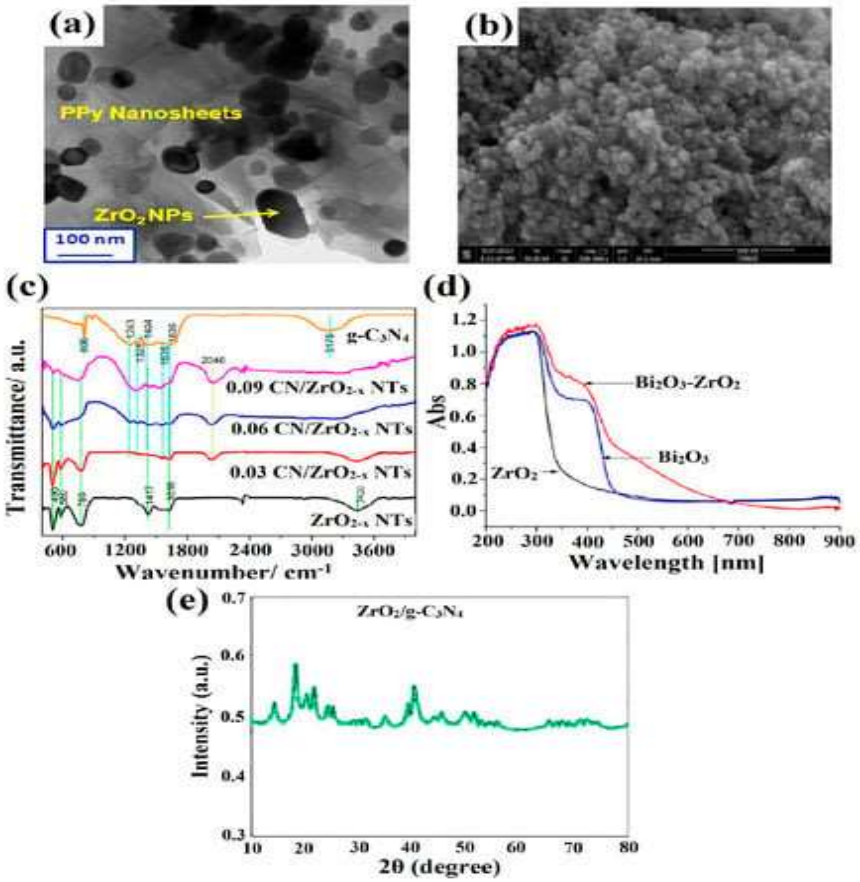


Figure 5. (**a**) HRTEM images and SAED pattern of ZrO_2/ PPy composite, reproduced with permission from Elsevier (License NO. 5333050908229) [53], (**b**) SEM images of calcined ZrO_2-$ZnCo_2O_4$ at 650 °C, reprinted with permission from Elsevier (License NO. 5333051169811) [61], (**c**) FTIR spectrum of g-C_3N_4, ZrO_2 NTs and g-C_3N_4/ZrO_{2-x} NTs, reprinted with permission from Elsevier (License NO. 5332980412880) [55], (**d**) UV-vis-DRS spectrum of Bi_2O_3-ZrO_2, Bi_2O_3, and ZrO_2, reproduced with permission from Elsevier (License NO. 5333060789631) [64], and (**e**) XRD pattern of 30 wt% ZrO_2/g-C_3N_4 (Zarei, 2020)

ZrO_2 Synthesis by Sol-Gel method:

Preparation of zirconium oxide nano particle:

Zirconium oxide nanoparticle is prepare via sol gel technique. Propanol (Sigma-Aldrich), water and ammonia solution (Systerm) are mix and stir for 5 minute. After that, Zirconium (IV) propoxide (sigma-Aldrich) is added and the solution is keep stirring for 1 hour. The resulting sol is then heated to 70°C to remove solvent and further dried in vacuum

Copyright to the author of some rights reserved This work is licensed under aCreative Commons Attribution-ShareAlike 4.0 International License.

International Journal of Business and Quality Research
https://e-journal.citakonsultindo.or.id/index.php/IJBQR
E-ISSN: 2985-9468

oven. The dried powder sample is then calcine in furnace with heating rate of 1°C per minute and remain 500°C peak temperature for 2 hour. The same method is repeated by replacing ammonia solution with nitric acid (Systerm) and a blank sample which synthesize without ammonia solution or nitic acid is also produced. The mole ratio of Zirconium propoxide, water and propanol is fixed at 1:8:20 and the mole ratio of ammonia solution and nitric acid to zirconium propoxide is vary from 0.2 till 0.8.

Sample characterization:

The calcined zirconium oxide nano particle powder produced are characterised by FTIR spectrophotometer (Perkin Elmer Spectrum BX) in the region of 400-4000 cm-1 as KBr pallets. X-ray diffraction are determined with Bruker D8 Advance and morphology of the sample is view by FESEM (Carl-Zeiss SUPRA 55VP) (Lim, Ahmad, & Hamzah, 2013).

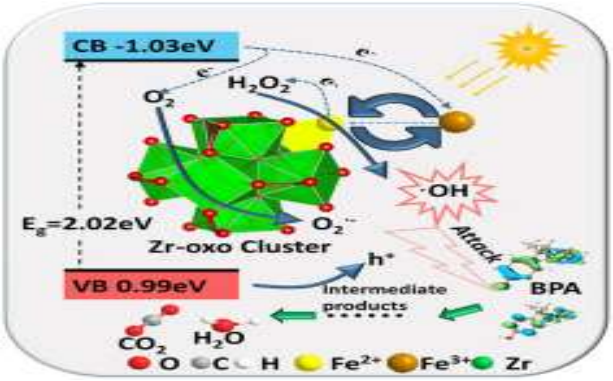
Zr based different Catalyst

Fe based Zr catalyst for BPA degradation:

To enhance the efficiency of photogenerated electron transport in the photo-Fenton reaction, we report a Fe-doped UiO-66 containing Fe–O–Zr bonds for the photo-Fenton reaction system. The modulation changes the energy bandgap from 3.89 eV to 2.02 eV, and its absorption edge is red-shifted from the UV region to the visible range. Simultaneously, Fe–O–Zr reduces the redox internal resistance, enhances the photocurrent and catalytic process, and suppresses the compounding of photogenerated electrons and holes. These promote the valence cycling of Fe(III)/Fe(II) in the photo-Fenton reaction. Compared with UiO-66, the hydroxyl radical generation efficiency of this reaction system was increased by 5.8 times (UiO-66: 0.0009 mM/min, FeUiO-1: 0.0053 mM/min). The degradation efficiency of BPA was increased by 100.8 times (UiO-66: 0.0012 min^{-1}, FeUiO-1: 0.121 min^{-1}), and the removal rate of TOC also reached 69.55%. The removal rate of BPA was maintained at more than 85% through 5 cycles. The reaction system was able to maintain a removal rate more than 97% at pH:3–9. In the presence of anions, such as Cl^-, SO_4^{2-}, NO_3^{2-} (10 mM), the degradation rates of BPA were still above 94%. The catalytic efficiency was 2.02 times higher under natural light than relative to dark conditions. It was demonstrated by EPR and inhibition experiments that the main active species in the reaction were hydroxyl radicals and vacancies. The HOMO energy level and LUMO energy level of the intermediates were analyzed, and the possible degradation pathways of the active species were speculated. Evaluation of the biological toxicity of intermediates demonstrated that the system can effectively detoxify BPA. This investigation provides a reference method to enhance the efficiency of the photo-Fenton reaction of MOFs (Zeyu Guan, 2022).

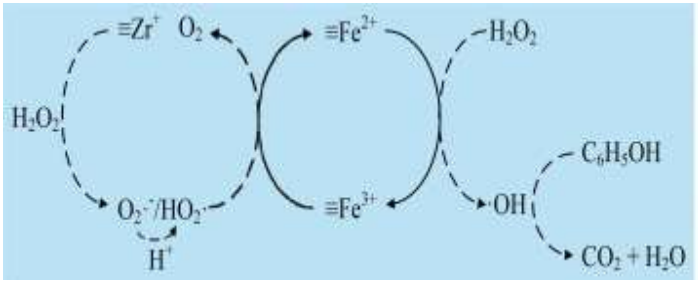
Copyright to the author of some rights reserved This work is licensed under aCreative Commons Attribution-ShareAlike 4.0 International License.

International Journal of Business and Quality Research
https://e-journal.citakonsultindo.or.id/index.php/IJBQR
E-ISSN: 2985-9468



Fe based Zr catalyst for Phenol degradation:

A novel Fe_2O_3-ZrO_2 catalyst was prepared by the sol-gel method, and investigated for phenol degradation in the Fenton-like reaction under neutral pH condition. The ZrO_2 addition increased the surface areas of the catalyst. Scanning electron microscopy (SEM) showed that ZrO_2 nano-particle dispersed on the surface of Fe_2O_3. X-ray photoelectron spectroscopy (XPS) indicated that the Fe^{2+} amount increased with the increase of the Zr content on the surface. The Fe_2O_3-ZrO_2 catalyst produced hydroxyl radicals (OH) and superoxide radicals (O_2^-/HO_2), and exhibited good catalytic performance in the reaction. Total phenol conversion and 56% TOC removal were achieved after 210 min under neutral pH at 60 °C in the heterogeneous Fenton-like reaction. In addition, the prepared Fe_2O_3-ZrO_2 catalyst had good magnetism (Pan Gao, 2018). An environment-friendly, effective and magnetic Fe_2O_3-ZrO_2 catalyst for phenol degradation in the Fenton-like reaction.





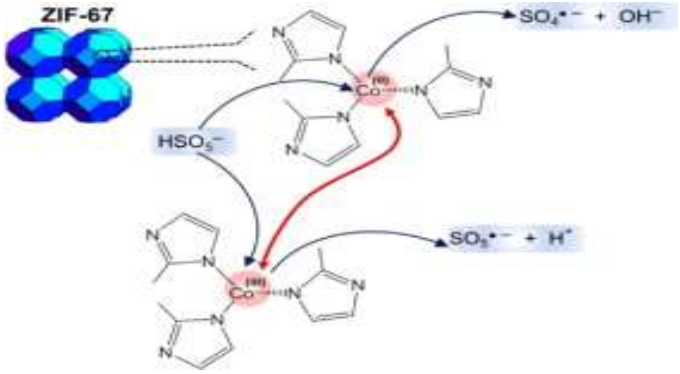
Co based Zr catalysts for Rhodamine B (RB) dye:

Metal organic frameworks (MOFs) can exhibit chemical, photo and biomimetic catalytic activities. While MOFs have been intensively investigated as photo-catalysts to degrade pollutants in water, studies of wet chemical oxidation catalyzed by MOFs are still quite limited. Particularly, the activation of peroxymonosulfate (PMS) represents a widely-

Copyright to the author of some rights reserved This work is licensed under aCreative Commons Attribution-ShareAlike 4.0 International License.

International Journal of Business and Quality Research
https://e-journal.citakonsultindo.or.id/index.php/IJBQR
E-ISSN: 2985-9468

used chemical oxidation reaction for chemical synthesis and environmental remediation. Yet little effort has been made to evaluate MOFs as a catalyst for the PMS activation. In this study, it is proposed to use a cobalt-based MOF, ZIF-67, as a heterogeneous catalyst to activate PMS to degrade Rhodamine B (RB) dye. Through the RB degradation, ZIF-67 as the PMS activation catalyst was evaluated and its underlying mechanism was proposed. Additionally, factors affecting the PMS activation were also examined, including ZIF-67 loading, temperature, pH, UV irradiation and ultrasonication. A ratio of 1/3/1 (RB/PMS/ZIF-67) is the most effective ratio to degrade RB in water. The higher temperature, UV irradiation and ultrasonication also enhanced the RB degradation using PMS activated by ZIF-67. The recyclability test revealed that ZIF-67 can be used continuously with stable and effective catalytic activity. These features reveal that ZIF-67 can be an interesting and promising heterogeneous catalyst to activate PMS for the degradation of organic pollutants in water (Kun-Yi Andrew Lin, 2015).



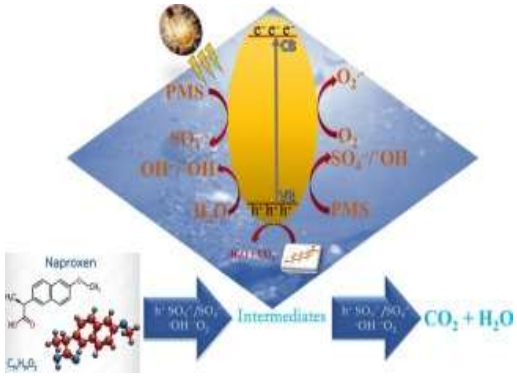
Mo based Zr catalyst:

Molybdenum carbide (Mo_2C), vanadium carbide (VC), and zirconium carbide (ZrC) nanoparticles (NPs) were investigated systematically as photocatalysts for the stimulation of peroxymonosulfate (PMS) for the degradation of naproxen (NX) under visible light. Characterizations of the samples by XRD, XPS, SEM, UV/PL, and BET were performed. In particular, the impact of exogenous variables on NX degradation was thoroughly and methodically investigated. 80.47 % of NX was decomposed over 60 min with 0.75 g/L PMS and ZrC at pH 3. ZrC NPs showed higher photocatalytic/photo-piezocatalytic properties in the degradation of NX compared to VC and Mo_2C NPs. The substantial rise in the reaction rate of NX in ZrC/PMS-based photo-degradation can be attributed to the larger surface area, mesoporous, narrow energy bandgap (E_g), and lower intensity of photoelectrons and holes recombining of ZrC NPs. Due to their substantial photocatalytic efficacy and significant piezo-photocatalytic properties, all NPs are viable candidates for piezo-photocatalytic/photocatalytic degradation. The degradation of NX was then seen in the

Copyright to the author of some rights reserved This work is licensed under aCreative Commons Attribution-ShareAlike 4.0 International License.

International Journal of Business and Quality Research
https://e-journal.citakonsultindo.or.id/index.php/IJBQR
E-ISSN: 2985-9468

active species scavenging studies, in which sulfate radicals, hydroxyl radicals, holes, and superoxide radicals were involved. According to continuous cycle studies, the ZrC NPs also had excellent durability and reusability. Additionally, the potential paths for NX degradation were proposed based on the study of LC-MS, and the degradation mechanism of NX was clarified. Based on the superior stability and reusability of ZrC NPs after 5 successive cycles, this material is anticipated to be utilized in the future for the treatment of wastewater, containing pharmaceuticals (Raqiqa Tur Rasool, 2023).



Applications of ZrO_2:

- ✓ ZrO_2 is a transition metal oxide and a prominent candidate for photocatalysis owing to its high refractive index, high corrosion resistance, and good photochemical stability, as well as optical absorption ability (Idrissi, Ziti, Labrim, & Bahmad, 2021).
- ✓ ZrO_2 is rich in OVs, which exist on the surface or in the lattice's interstitial sites, which further promotes the optoelectronic properties of ZrO_2 leading to boosted light harvesting ability and superior isolation of photocarriers (Wahba, Yakout, Mohamed, & Galal, 2020).
- ✓ The optical characteristics of ZrO_2 are modified by the introduction of midgap states in the elemental doping, resulting in optimal visible light responsive photocatalyst [22]. By doping with ZrO_2, ions diffuse throughout the lattice at interstitial sites, resulting in a new valance band maximum (VBM) or conduction band minimum (CBM), which narrows the optical bandgap of ZrO_2 (Faizan, Siddique, Ahmad, Tripathi, & Riyajuddin, 2021).

Application of Zr-based in PMS based degradation:

Advanced oxidation processes (AOPs), which rely on the generation of extremely reactive and thus highly unstable radical species (e.g., $SO_4^{\bullet-}$, •OH, etc.) from certain redox-active chemicals (e.g., H_2O_2, PMS), have become state-of-the-art water treatment

Copyright to the author of some rights reserved This work is licensed under aCreative Commons Attribution-ShareAlike 4.0 International License.

International Journal of Business and Quality Research
https://e-journal.citakonsultindo.or.id/index.php/IJBQR
E-ISSN: 2985-9468

technologies for the elimination of organic micropollutants Hodges et al., 2018; Li et al., 2020; Zhang et al., 2022). Various strategies such as energy-input (e. g., heat, UV) (Wen et al., 2022), carbon-based materials (Duan et al., 2014), transition metals (Chen et al., 2022; Yang et al., 2019), etc., can be used to activate the oxidants to generate these reactive radical species. Among these approaches, transition metals with variable valent states and unoccupied 3d orbitals, such as Fe, Co, Mn, Cu, etc., are generally regarded as the most effective activators (Guo et al., 2021; Ren et al., 2020b; Xu et al., 2021). Transient metals can promote the decomposition of oxidants to radicals through the $M^{n+}/M^{(n+1)+}$ redox cycling, during which the reduction of $M^{(n+1)+}$ to M^{n+} is usually the rate-limiting step (Guo et al., 2022; Hodges et al., 2006; Song et al., 2022). Meanwhile, the reduction of high-valent metal species comes with the cost of oxidants decomposition without generating highly reactive radicals (Eqs. (1) and (2)), thus lowering the utilization efficiency of oxidants (Lyu et al., 2018; Mi et al., 2022). Therefore, an economical and high-efficient metal catalyst that does not depend on its redox cycling is highly desired.

$$\mathbf{M_{surface}^{(n+1)+} + H_2O_2 \rightarrow M_{surface}^{n+} + OOH^{\bullet} + H^+}$$

$$\mathbf{M_{surface}^{(n+1)+} + OOH^{\bullet} \rightarrow M_{surfacen}^{+} + O_2 + H^+}$$

Zirconium dioxide (ZrO_2) is a popular ceramic material. It has attracted increasing attention in various fields owing to its unique merits of low toxicity, easy synthesis, strong stability and excellent biocompatibility (Chen et al., 2020; Zhang et al., 2019). Applications of ZrO_2 in wastewater treatment have been reported. For example, ZrO_2, especially amorphous ZrO_2, can act as the absorbent to remove anions in water, such as fluoride (Pan et al., 2013), arsenate (Moraga et al., 2019), and phosphate (Su et al., 2013), because they can strongly complex to the Zr sites. Note that, in heterogeneous Fenton-like oxidation processes, the first step is usually the complexation between the transient metals and the oxidant anions (e.g., HSO_5^-, $S_2O_8^{2-}$, HO_2^-) (Hu et al., 2017; Li et al., 2021). Nevertheless, owing to the redox-inert nature of ZrO_2, little attention has been paid to its potential catalytic activity in Fenton-like reaction processes. So far, the application of ZrO_2 in AOPs is limited to its role of an inert carrier of catalysts (Yin et al., 2021).

Recent studies indicated that ZrO_2 could activate H_2O_2 to generate radicals. For example, Ziolek *et al*. reported that d^0 transition-metal oxides (e.g., ZrO_2, Ta_2O_5, Nb_2O_5) with acidic-base surface functional groups could induce the decomposition of H_2O_2 to generate radicals (Ziolek et al., 2015). Unlike conventional Fenton-like processes, no interfacial electron transfer occurred in this process. Sobańska et al. (2017) further found that amorphous ZrO_2 ($aZrO_2$) showed peroxidase-like activity at pH < IEP (Eq. (3)); it could decompose H_2O_2 to form •OH and $O_2^{\bullet-}$. At pH > IEP, however, it showed catalase-like (Eq.

Copyright to the author of some rights reserved This work is licensed under aCreative Commons Attribution-ShareAlike 4.0 International License.

International Journal of Business and Quality Research
https://e-journal.citakonsultindo.or.id/index.php/IJBQR
E-ISSN: 2985-9468

(4)) activity that decomposed H_2O_2 to O_2. In the proposed mechanism, the electrons were only transferred from the H_2O_2 in the bulk solution to the adsorbed HO_2^-. During this process, the $aZrO_2$ served as an ionic sponge where the charged $O_2^{\bullet-}$ and O_2^{2-} species and protons could be stabilized and accumulated on the surface. Our recent study has also demonstrated that the abundant hydroxyl groups on the surface of $aZrO_2$ could induce the intermolecular electron transfer, thereby promoting the production of $HO_2^{\bullet}/O_2^{\bullet-}$ (Yin et al., 2021). Such a pathway does not involve the redox reaction of the Zr metals, which is distinct from conventional Fenton-like processes and would greatly increase the utilization efficiency of oxidants. However, these studies are still in their infancy, and only few studies on glycerol oxidation have been reported (Sobańska et al., 2017). It is still unclear whether it can be used to degrade organic contaminants in wastewater. The key reactive species and the intrinsic mechanisms also remain ambiguous, which deserves further investigations.

$$HO_{2(ads)}^- + H_2O_{2(aq)} \rightarrow {}^{\bullet}OH_{(aq)} + O_{2(ads)}^{-\bullet} + H_2OH_2O_{2(aq)} \rightarrow 12O_{2(g)} + H_2O$$

Herein, we demonstrated for the first time that amorphous phase ZrO_2 prepared via a modified precipitation method could effectively activate PMS to degrade organic contaminants. Distinct from conventional activated PMS oxidation processes, the $aZrO_2$/PMS system showed extraordinarily high utilization efficiency of PMS and unique oxygen-atom-transfer pathway with selected molecules. The $aZrO_2$-activated PMS complex (Zr(IV)-PMS*), rather than free radicals, was identified as the principal reactive species in the $aZrO_2$/PMS system. DFT computation was employed to rationalize the mechanisms of Zr(IV)-PMS* complex formation. Overall, the $aZrO_2$/PMS system shows great promise to address the organic micropollutants in complex water matrix.

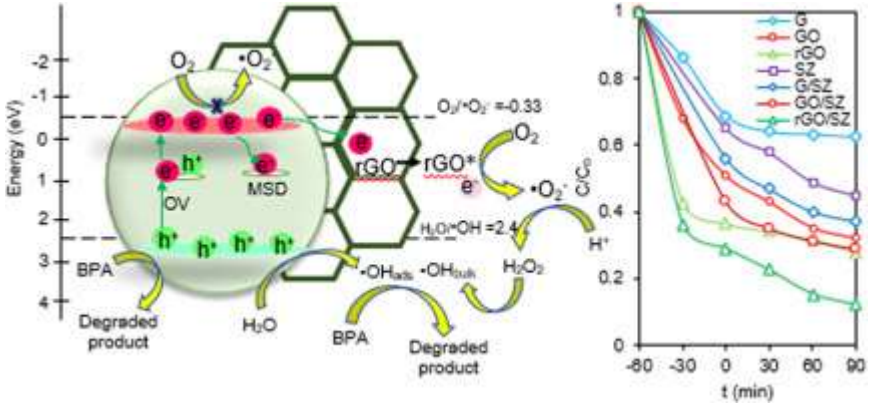
BPA Degradation Zirconia composites:

Bisphenol A (BPA) is an endocrine disruptor, and removing it from contaminated water is a major environmental concern. Herein, graphene derivatives such as graphene (G), graphene oxide (GO), and reduced graphene oxide (rGO) supported silica-zirconia (SZ) were successfully synthesized for photodegradation of BPA. The photodegradation of BPA was ordered as follows: rGO/SZ (88%)>GO/SZ (63%)>G/SZ (58%)>SZ (55%). This is because rGO has bigger regions for π-π stacking and less negatively charged carboxyl groups, which BPA has a higher adsorption affinity than GO. In addition, the highest degradation is predominantly due to the high number of carbon-support interactions and defects sites, including oxygen vacancy. This encouraged effective mobility of charge carriers and subsequently enhanced photoactivity. In this study, the rGO/SZ catalyst was

Copyright to the author of some rights reserved This work is licensed under aCreative Commons Attribution-ShareAlike 4.0 International License.

International Journal of Business and Quality Research
https://e-journal.citakonsultindo.or.id/index.php/IJBQR
E-ISSN: 2985-9468

chosen to optimize further the reaction parameters including catalyst dosage, pH and initial concentration of BPA. According to the analysis of variance, the catalyst dosage was the most important variable in the degradation of BPA, followed by pH and initial concentration. The optimum BPA degradation predicted from response surface methodology is 88% at conditions of 8.09 mg L^{-1} using 0.469 g L^{-1} of rGO/SZ at pH 6.1, which is reasonably close to the predicted value (89.8%). The rGO/SZ catalyst was found to be stable even after five cycles in the reusability testing (N.S. Hassan, 2021).



A $ZnFe_2O_4$-TiO_2 nanocomposite combining p-type $ZnFe_2O_4$ and n-type TiO_2 was successfully fabricated. The $ZnFe_2O_4$-TiO_2 nanocomposite greatly enhanced the bisphenol A (BPA) photodegradation under visible light irradiation at 465 ± 40 nm. Loading TiO_2 with 1 wt% of $ZnFe_2O_4$ produced high photocurrent and low charge transfer resistance. The photodegradation rate of BPA by $ZnFe_2O_4$-TiO_2, which was highly dependent on the water chemistry including pH, anions, and humic acid, was 20.8-21.4 times higher than that of commercial TiO_2 photocatalysts. Chloride and sulfate ions enhanced BPA photodegradation mostly due to the production of more radical species; whereas nitrate, dihydrogen phosphate, and bicarbonate ions decreased the photodegradation rate of BPA due to the scavenge of hydroxyl radicals. The photoactivity and recyclability of $ZnFe_2O_4$-TiO_2 in lake water was also assessed. A near complete BPA removal from lake water was observed under visible light irradiation. Furthermore, >90% of photocatalytic activity toward BPA degradation was achieved in 5 cycles of continuous addition of BPA to the lake water. The BPA degradation intermediates were identified by HPLC/MS/MS and possible reaction pathways were proposed. Results clearly demonstrate the excellent visible-light-sensitive photocatalytic degradation of BPA over ZnFe2O4-TiO2 composite which has a great application potential for the decomposition of emerging contaminants in impaired waters (Binh Nguyen, 2018).

Copyright to the author of some rights reserved This work is licensed under aCreative Commons Attribution-ShareAlike 4.0 International License.

International Journal of Business and Quality Research
https://e-journal.citakonsultindo.or.id/index.php/IJBQR
E-ISSN: 2985-9468

Degradation of Ciprofloxacin by ZrO_2 Composites:

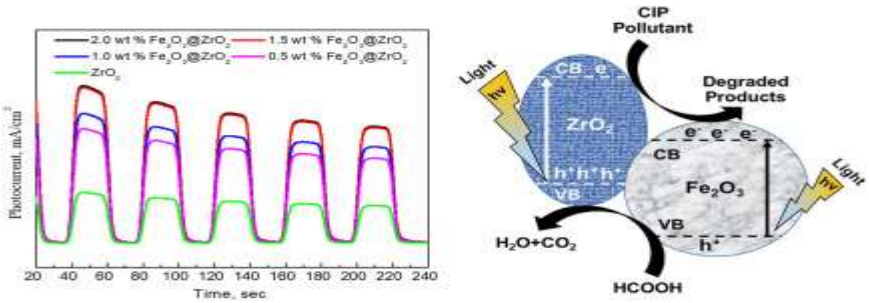
Aquatic ecology has been greatly threatened by the discharge of effluents of textile and antibiotic industries into natural waters. Herein, an efficient and easily recycled reduced graphene oxide/zirconium oxide nanocomposite has been synthesized using banana peel extract (abbreviated as rGO-ZrO_2 in this work). The X-ray diffraction (XRD), field emission scanning electronic microscopy (FESEM), high-resolution transmission electron microscopy (HRTEM), Brunauer-Emmett-Teller (BET), UV-visible diffuse reflectance spectroscopy (DRS), X-ray photoelectron spectroscopy (XPS), and Fourier transform infrared (FTIR) spectroscopy were used to analyze the synthesized material. The as-prepared rGO-ZrO_2 nanocomposite was employed as a photocatalyst for the decomposition of rhodamine blue (RhB) and crystal violet (CV) dyes, and ciprofloxacin (CIP) antibiotic by illumination with direct sunlight. The RhB and CV were degraded to maximum extent of around 86 and 90%, respectively, over the rGO-ZrO_2 nanocomposite after exposure to direct sunlight for 120 min. On the other hand, the degradation of CIP was approximately 93.1% over the rGO-ZrO_2 nanocomposite in 240 min under same experimental conditions. Further studies were performed regarding the role of parameters like pH, catalyst dose, and scavengers, in order to understand the superiority of rGO-ZrO_2 nanocomposite in degrading organic pollutants. Moreover, the intermediate products and plausible CIP degradation mechanisms were examined using liquid chromatography-mass spectrometry (LC-MS). Moreover, the catalyst was easily separated from the solution and demonstrated good stability and reusability. The RhB, CV, and CIP removal efficiency were 80%, 83%, and 88%, respectively, after five cycles (Kaushal S, 2023).

Ciprofloxacin (CIP) remediation has been carried out using Fe_2O_3@ZrO_2 nanocomposites, which were fabricated by means of easy wet chemical approach by combining mesoporous ZrO_2 and Fe_2O_3 with varied concentrations and used in this study. The crystal structure, composition, morphology, electrical and optical features of the prepared materials were checked via different techniques. The gained results indicated the possibility of Fe_2O_3 to be doped into the ZrO_2 structure. Furthermore, the gained TEM images revealed that the Fe_2O_3 nanoparticles were spherical and uniformly scattered inside the ZrO_2 nanoparticles. The Fe_2O_3@ZrO_2 nanocomposites were investigated as a new effective photocatalyst against CIP remediation using visible light. A faultless crystalline structure, a great surface area, a small bandgap with decreasing recombination between induced charges, a mesoporous structure of Fe_2O_3@ZrO_2 nanocomposites photocatalyst were all factors that contributed to the increased efficiency. Fe_2O_3@ZrO_2 nanocomposites containing 1.5 wt% Fe_2O_3 improved the photocatalytic CIP remediation effectiveness from 35% to 100% in within 60 min. Even after

Copyright to the author of some rights reserved This work is licensed under aCreative Commons Attribution-ShareAlike 4.0 International License.

International Journal of Business and Quality Research
https://e-journal.citakonsultindo.or.id/index.php/IJBQR
E-ISSN: 2985-9468

five cycles of application, the recycled Fe_2O_3@ZrO_2 nanocomposite exhibited such a change with excellent performance and no decrease in efficiency. Using visible light, the created Fe_2O_3@ZrO_2 nanocomposite could be used as an environmentally friendly photocatalyst to remediate pollutants with minimal energy (Majdah.Raji.M. Alotaibi, 2022).



Methylene Blue (MB) And Rhodamine B (Rhb) Dyes Degradation:

Wastewater management is the most discussed topic in this current era. To overcome the scarcity of water and wastewater treatment, reusage of water is the convenient way. By removing the organic pollutants, the water can be reused for domestic purposes. Pure and neodymium (Nd) doped ZrO_2 was produced using facile co-precipitation technique. Along with doping, surfactant was also included to enhance the morphology of the prepared samples. The nanoparticles morphology was formed with less agglomeration as investigated by TEM analysis. The photocatalytic action was further examined using annular photoreactor. Both methylene blue (MB) and Rhodamine B (RhB) dyes degradation was examined. Neodymium doped ZrO_2 was incorporated in the dye under visible light for 2 h. The light was irradiated for 20 min and sample solution was collected for every 20 min. The samples were analyzed for UV and degradation was confirmed. The enhancement of catalyst depended on the bandgap of the samples. The absorption peak for Rhodamine B and Methylene Blue dyes at 553 and 664 nm was decreased and confirmed the degradation of dyes. 2% Nd doped ZrO_2 catalyst added MB dye sample showed 90% efficiency and exhibited 77% efficiency on Rhodamine B pollutant. The "k" values of 2% Nd doped ZrO_2 was obtained as 0.0144 min^{-1} and 0.00944 min^{-1} for MB and RhB dyes. This candidate will be the potential one for futuristic water remediation process (S.P. Keerthana, 2022).

Photodegradation and Its Mechanism:

Environmental contamination by organic dyes, pharmaceuticals, and insecticides is posing a serious threat worldwide owing to their toxic, cancerous nature and difficulty in total decomposition causing a shortage in drinking water. Thus far, various traditional procedures, including biological, physical, and chemical methods have been used to remove

Copyright to the author of some rights reserved This work is licensed under aCreative Commons Attribution-ShareAlike 4.0 International License.

International Journal of Business and Quality Research
https://e-journal.citakonsultindo.or.id/index.php/IJBQR
E-ISSN: 2985-9468

these pollutants, however the applicability of these technologies is limited due to their high cost, risk of hazardous byproducts, and poor efficiency. As a result, a more direct and effective way to deal with these contaminants is highly essential (Zhao, et al., 2022). Water treatment employing a simple method like photocatalysis is in the limelight owing to its low energy requirement, cost-effectiveness, capacity to adsorb a wide range of natural and inorganic substances on the photocatalyst's surface, and complete degradation without hazardous by-products (Xu, et al., 2021). Even photocatalysis seemed to be a promising method due to the easy availability of a large amount of solar energy. Semiconductor photocatalytic activity has potential applications in the degradation of environmental contaminants and pollutant transformation. Thus, it has aroused a lot of attention (Pirzada, et al., 2015).

Organic Pollutant Degradation:

Organic pollutants are identified as harmful for human health as they are toxic, carcinogenic, and teratogenic, so the use of heterogeneous photocatalysis to decontaminate wastewater containing organic compounds is an attractive solution to the effluent treatment problem since it brings about chemical degradation into non-toxic molecules like carbon dioxide and water (Zhao, et al., A critical review on surface modified nano-catalysts application for photocatalytic degradation of volatile organic compounds, 2022). Charge transfer and electron transfer are involved in the degradation of organic pollutants, and these processes are impacted by the presence of charged species. The alluring features of ZrO_2 involving physicochemical stability and distinctive band structures render optimal photodegradation ability, however the broad bandgap and low separation rate of photocarriers limit its wide-scale practical uses (Chen, et al., 2020). However, the synergistic coupling of ferrites with zirconia boosts the overall photoactivity by the combined action of inhibited charge separation and integration of photo and Fenton activity. In detail, **Figure 6**a depicts the suggested photocatalytic process on the $ZrO_2/ZnFe_2O_4$ nanocomposite (ZZFO 12 NC) for the photodegradation of indigo carmine dye (98%) (Renuka, et al., 2021). After the excitation and isolation of photocarriers, the reaction of photoinduced electrons oxygen yielded superoxide radicals ($\bullet O_2^-$), which further reacted with H_2O to produce H_2O_2. This generated H_2O_2 reaction with α-Fe_2O_3 in ZZFO 12 further produced •OH radicals and participated in dye degradation, as shown in Equations (1)–(7)

$$ZZFO + h\nu \rightarrow ZrO_2 - h^+ + ZnFe_2O_4 - e_{-} \quad (1)$$

$$ZnFe_2O_4 - e + O^{\bullet}{}_2 \rightarrow {}^{\bullet}O_{-2} \quad (2)$$

Copyright to the author of some rights reserved This work is licensed under aCreative Commons Attribution-ShareAlike 4.0 International License.

International Journal of Business and Quality Research
https://e-journal.citakonsultindo.or.id/index.php/IJBQR
E-ISSN: 2985-9468

$$\cdot O_{-2} + H_2O \rightarrow H_2O_2 + \cdot OH \quad (3)$$

$$H_2O_2 + \alpha - Fe_2O_3 \rightarrow 2\ \cdot OH \quad (4)$$

$$h^+ + OH^- \rightarrow 2\ \cdot OH \quad (5)$$

$$\cdot OH + \text{indigo carmine} \rightarrow \text{Degradation} \quad (6)$$

$$\cdot O^-_2 + \text{indigo carmine} \rightarrow \text{Degradation} \quad (7)$$

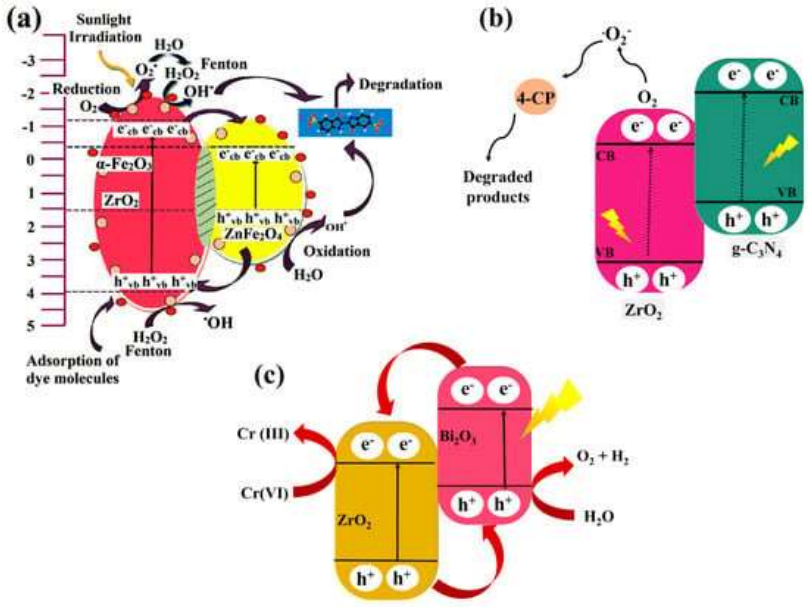


Figure 6. (**a**) Photodegradation pathway of indigo carmine dye under sunlight exposure for $ZrO_2/ZnFe_2O_4$ composite, reprinted with permission from Elsevier (License NO. 5333060926293) (Renuka, et al., 2021)(**b**) schematic representation of charge carriers' separation on 30 wt% ZrO_2/g-C_3N_4 composites under light illumination [65], and (**c**) systematic presentation of photocarriers transfer in Bi_2O_3-ZrO_2 hybrid in presence of visible light, reproduced with permission from Elsevier (Zarei, Ultrasonic-assisted preparation of ZrO2/g-C3N4 nanocomposites with high visible-light photocatalytic activity for degradation of 4-chlorophenol in water, 2020)(License NO. 5333060789631).

Other than dyes, phenolic compounds have also been treated effectively with ZrO_2-based nanocomposites. For example, ZrO_2/g-C_3N_4 nanocomposite synthesized by

Copyright to the author of some rights reserved This work is licensed under aCreative Commons Attribution-ShareAlike 4.0 International License.

International Journal of Business and Quality Research
https://e-journal.citakonsultindo.or.id/index.php/IJBQR
E-ISSN: 2985-9468

ultrasonication method for the efficient degradation of 4-chlorophenol (4-CP) (Figure 6b) in water with the highest degradation rate of 0.0173 min^{-1} [65]. The synergistic action of higher surface area with exposed active sites facilitates the adsorption of 4-CP and the surface-induced charges accelerated the formation of $\bullet O_2^-$ radicals which boosted the degradation efficiency. Moreover, from the radical scavenging results, it was confirmed that $\bullet O_2^-$ radicals and h+ primarily participated in the degradation process (Zarei et al; 2020).

Inorganic Pollutant Degradation:

The higher concentration of inorganic pollutants in the water due to their discharge from various industries like fertilizers, refineries, and pharmaceuticals is causing a major threat to human as well as aquatic lives. Thus, the photocatalytic treatment of such toxic effluents using ZrO_2 as a photocatalyst can be a potential solution. In this regard, enhancement in Cr (VI) photoreduction under visible light irradiation is achieved by developing a Bi_2O_3-ZrO_2 nanocomposite [64]. Bi_2O_3-ZrO_2 has a greater photocatalytic activity (92.30%) after an irradiation period of 180 min. The mechanism for enhanced photocatalytic activity of Bi_2O_3-ZrO_2 is explained according to previously published literature on the photocatalytic activity of nanocomposites. Typically, Cr (VI) is photo-reduced by CB electrons captured by ZrO_2, and the VB holes further oxidized H_2O to create O_2 (Figure 6c). The detailed photocatalytic processes that occur on the surface of Bi_2O_3-ZrO_2 are summarized in Equations (8)–(11):

$$Bi_2O_3 + hv \rightarrow Bi_2O_3(h^+_{VB} + e^-_{CB}) \quad (8)$$

$$Bi_2O_3(e^-_{CB}) + ZrO_2 \rightarrow Bi_2O_3 + ZrO_2(e^-_{CB}) \quad (9)$$

$$ZrO_2(6e^-_{CB}) + Cr_2O^{2-}_7 + 14H^+ \rightarrow 2Cr_3^+ + 7H_2O + ZrO_2 \quad (10)$$

$$2H_2O + 4h^+ \rightarrow O2 + 4H^+ \quad (11)$$

Various ZrO_2-based semiconductor photocatalysts with incremented photodegradation activity are summarized in Table 1

Photocatalyst	Enhancement Strategies	Reaction Parameter	Targeted Pollutant	Photocatalyst Efficiency	Ref.
Ni doped ZrO_2	Doping	Visible light lamp (>400	Methylene blue	90.2% in 100 min.	[59]

Copyright to the author of some rights reserved This work is licensed under aCreative Commons Attribution-ShareAlike 4.0 International License.

International Journal of Business and Quality Research
https://e-journal.citakonsultindo.or.id/index.php/IJBQR
E-ISSN: 2985-9468

		nm), 15 mg photocatalyst			
C-doped ZrO_2	Doping	PL-L lamp, 0.2 g/L photocatalyst	Methylene blue	75%	[70]
Nd doped ZrO_2	Doping	pH = 7	Methylene blue, Rhodamine B, and acetophenone	90%, 77%, and 60%	[71]
Al_2O_3/ZrO_2	Heterojunction	Visible light, 0.04 g catalyst	Reactive blue 222 and Reactive yellow 145	91.4% and 94.6% in 60 min.	[72]
RE/ZrO_2 (RE = Sm, Eu)	Heterojunction	350 W Xenon lamp	Methylene blue and Rhodamine B	100% in 30 min. and 96.3% in 90 min.	[73]
ZnO QDs@ZrO_2-TiO_2	Heterojunction	Ultra violet light	Congo Red	94.62%	[74]
ZrO_2/Dy_2O_3	Heterojunction	Xenon lamp with cut-off UV filter	Rhodamine B, and Methylene blue	100% in 30 min. and 87.79%	[75]
TiO_2-ZrO_2	Heterojunction	125 W Mercury lamp, pH = 7.6, 10 mg/L photocatalyst	Metformin	92% in 150 min.	[76]
g-C_3N_4/ZrO_2	Heterojunction	50 W LED lamp, 30 mg photocatalyst	Methylene blue, Rhodamine B, Congo Red,	96%, 98%, 90%, and 83%	[77]

Copyright to the author of some rights reserved This work is licensed under aCreative Commons Attribution-ShareAlike 4.0 International License.

			and Tetracycline		
$CuCo_2O_4$@ZrO_2	Heterojunction	Visible light	Tetracycline	95%	[78]
TiO_2/ZrO_2	Heterojunction	100 W LED lamp	Rhodamine B	90%	[79]

Summary of various ZrO_2-based semiconductor photocatalysts for the incremented photocatalytic degradation of aqueous phase pollutants (Reddy, et al., 2020), (de Moraes, de Azeredo, Bacetto, da Silva, & Rodrigues, 2018), (Yaghoubi, Ramazani, & Taghavi Fardood, 2020) & (Tanzifi, Jahanshahi, Peyravi, & Khalili, 2022).

Future Direction:

In summary, various techniques have been utilized to enhance the efficiency of zirconium dioxide such as doping, metal loading. Although co-catalysts have gained a lot of interest by researchers, more efforts should be directed in strengthening the binding force between the co-catalyst and the semiconductor. Moreover, high cost of noble metals, aggregation and corrosion can be overcome by replacing the noble metals with cheap transition metals; thus, more investigation is required in that field (E.M. Sharaf Aldeen, 2022).

REFERENCES

Ahmed, W., & Iqbal, J. (2020). Co doped ZrO2 nanoparticles: An efficient visible light triggered photocatalyst with enhanced structural, optical and dielectric characteristics. *Ceram. Int*, 25833–25844.

Aldeen, E., Jalil, A., Mim, R., Alhebshi, A., Hassan, N., & Saravanan, R. (2022). Altered zirconium dioxide based photocatalyst for enhancement of organic pollutants degradation: A review. *Chemosphere* , 135349.

Binh Nguyen, C. H.-a. (2018). Photocatalytic degradation of bisphenol A over a ZnFe 2 O 4 /TiO 2 nanocomposite under visible light. *The Science of The Total Environment 646*.

Camila M. Loffredo, M. D. (2023). Fe-Mn/ZrO2 catalysts: Sulfate-based-advanced oxidation process for the degradation of olive oil industry model pollutants. *Catalysis Communications*, 106578.

Camila M. Loffredo, M. D. (2023). Fe-Mn/ZrO2 catalysts: Sulfate-based-advanced oxidation process for the degradation of olive oil industry model pollutants. *Catalysis Communications*, 106578.

Copyright to the author of some rights reserved This work is licensed under aCreative Commons Attribution-ShareAlike 4.0 International License.

Chen, Q., Yang, W., Zhu, J., Fu, L., Li, D., & Zhou, L. (2020). Enhanced visible light photocatalytic activity of g-C3N4 decorated ZrO2−x nanotubes heterostructure for degradation of tetracycline hydrochloride. *J. Hazard. Mater*, 384, 121275.

Dang, V. Q., & Al-Ali, K. (2020). The synthesis and investigation of the reversible conversion of layered ZrS 2 and ZrS 3. New Journal of Chemistry, 44(18), 7583-7590.

de Moraes, N., de Azeredo, C., Bacetto, L., da Silva, M., & Rodrigues, L. (2018). The effect of C-doping on the properties and photocatalytic activity of ZrO2 prepared via sol-gel route. *Optik* , 165, 302–309.

E.M. Sharaf Aldeen, A. J. (2022). Altered zirconium dioxide based photocatalyst for enhancement of organic pollutants degradation: A review. *Chemosphere*, 135349.

Faizan, M., Siddique, M., Ahmad, S., Tripathi, P., & Riyajuddin, S. (2021). Tunable luminescence in Ce3+/Mn2+ co-doped ZrO2 nanophosphor integrated with theoretical studies on possible (ZrO2) n clusters using DFT method. *J. Alloys Compd*, 157378.

Idrissi, S., Ziti, S., Labrim, H., & Bahmad, L. (2021). Sulfur doping effect on the electronic properties of zirconium dioxide ZrO2. *Mater. Sci. Eng. B* , 115200.

Jaenicke, S., Chuah, G. K., Raju, V., & Nie, Y. T. (2008). Structural and morphological control in the preparation of high surface area zirconia. *Catalysis surveys from Asia*, *12*, 153-169.

Katea, S. N., Riekehr, L., & Westin, G. (2021). Synthesis of nano-phase ZrC by carbothermal reduction using a ZrO2–carbon nano-composite. Journal of the European Ceramic Society, 41(1), 62-72.

Kaushal S, K. V. (2023). Sunlight-driven photocatalytic degradation of ciprofloxacin and organic dyes by biosynthesized rGO-ZrO2 nanocomposites. *Environ Sci Pollut Res Int*, 30(24):65602-65617.

Kun-Yi Andrew Lin, H.-A. C. (2015). Zeolitic Imidazole Framework-67 (ZIF-67) as a heterogeneous catalyst to activate peroxymonosulfate for degradation of Rhodamine B in water. *Journal of the Taiwan Institute of Chemical Engineers*, 40-45.

Lim, H. S., Ahmad, A., & Hamzah, H. (2013, November). Synthesis of zirconium oxide nanoparticle by sol-gel technique. In AIP Conference Proceedings (Vol. 1571, No. 1, pp. 812-816). American Institute of Physics.

Ma, H., He, Y., Chen, P., Wang, H., Sun, Y., Li, J., . . . Sheng, J. (2021). Ultrathin Two-Dimensional Bi-Based photocatalysts: Synthetic strategies, surface defects, and reaction mechanisms. *Chem. Eng. J*, 417, 129305.

Majdah.Raji.M. Alotaibi, M. M. (2022). Photocatalytic remediation of ciprofloxacin based on Fe2O3@ZrO2 nanocomposites under visible-light. *Optical Materials*, 112041.

Copyright to the author of some rights reserved This work is licensed under aCreative Commons Attribution-ShareAlike 4.0 International License.

N.S. Hassan, A. J. (2021). Photodegradation of bisphenol A from aqueous solution over reduced graphene oxide supported on tetragonal silica-zirconia nanocatalysts: Optimization using RSM. *Process Safety and Environmental Protection*, 496-507.

Pan Gao, Y. S. (2018). An effective and magnetic Fe2O3-ZrO2 catalyst for phenol degradation under neutral pH in the heterogeneous Fenton-like reaction. *Separation and Purification Technology*, 238-243.

Parveen, A., & Surumbarkuzhali, N. (2020). Spatial separation of photo-generated carriers and enhanced photocatalytic performance on ZrO2 catalysts via coupling with PPy. *Inorg. Chem. Commun*, 120, 108153.

Pelosato, R., Bolognino, I., Fontana, F., & Sora, I. (2022). Applications of Heterogeneous Photocatalysis to the Degradation of Oxytetracycline in Water: A Review. *Molecules* , 2743.

Pirzada, B., Mir, N., Qutub, N., Mehraj, O., Sabir, S., & Muneer, M. (2015). Synthesis, characterization and optimization of photocatalytic activity of TiO2/ZrO2 nanocomposite heterostructures. *Mater. Sci. Eng. B* , 193, 137–145.

Rani, V. A. (2022). ZrO2-Based Photocatalysts for Wastewater Treatment: From Novel Modification Strategies to Mechanistic Insights. *Catalysts* , 1418.

Raqiqa Tur Rasool, G. A.-S. (2023). Peroxymonosulfate-based photodegradation of naproxen by stimulating (Mo, V, and Zr)-carbide nanoparticles. *Journal of Water Process Engineering*, 104027.

Rashid, J., Barakat, M., Mohamed, R., & Ibrahim, I. (2014). Enhancement of photocatalytic activity of zinc/cobalt spinel oxides by doping with ZrO2 for visible light photocatalytic degradation of 2-chlorophenol in wastewater. *J. Photochem. Photobiol*, 284, 1–7.

Reddy, C., Reddy, I., Ravindranadh, K., Reddy, K., Kim, D., & Shim, J. (2020). Ni-dopant concentration effect of ZrO2 photocatalyst on photoelectrochemical water splitting and efficient removal of toxic organic pollutants. *Sep. Purif. Technol*, 252, 1173.

Renuka, L., Anantharaju, K., Vidya, Y., Nagabhushana, H., Uma, B., Malini, S., . . . Koppad, P. (2021). Porous network ZrO2/ZnFe2O4 nanocomposite with heterojunction towards industrial water purification under sunlight: Enhanced charge separation and elucidation of photo-mechanism. *Ceram. Int*, 47, 14845–14861.

Štefanić, G., Štefanić, I. I., & Musić, S. (2000). Influence of the synthesis conditions on the properties of hydrous zirconia and the stability of low-temperature t-ZrO2. *Materials Chemistry and Physics*, *65*(2), 197-207.

S.P. Keerthana, R. Y. (2022). Nd doped ZrO2 photocatalyst for organic pollutants degradation in wastewater. *Environmental Technology & Innovation*, 102851.

Copyright to the author of some rights reserved This work is licensed under aCreative Commons Attribution-ShareAlike 4.0 International License.

Siting Shao, J. C. (2022). Rapid pollutant degradation by peroxymonosulfate via an unusual mediated-electron transfer pathway under spatial-confinement. *RSC Advances*, 9.

Tanzifi, M., Jahanshahi, M., Peyravi, M., & Khalili, S. (2022). A morphological decoration of g-C3N4/ZrO2 heterojunctions as a visible light activated photocatalyst for degradation of various organic pollutants. *J. Environ. Chem. Eng*, 10, 108600.

Wahba, M., Yakout, S., Mohamed, W., & Galal, H. (2020). Remarkable photocatalytic activity of Zr doped ZnO and ZrO2/ZnO nanocomposites: Structural, morphological and photoluminescence properties. *Mater. Chem. Phys*, 123754.

Xia X, Z. F. (2020). A Review Study on Sulfate-Radical-Based Advanced Oxidation Processes for Domestic/Industrial Wastewater Treatment: Degradation, Efficiency, and Mechanism. *Front. Chem*, 592056.

Xu, F., Lai, C., Zhang, M., Li, B., Liu, S., Chen, M., . . . Fu, Y. (2021). Facile one-pot synthesis of carbon self-doped graphitic carbon nitride loaded with ultra-low ceric dioxide for high-efficiency environmental photocatalysis: Organic pollutants degradation and hexavalent chromium reduction. *J. Colloid Interface Sci*, 601, 196–208.

Yaghoubi, A., Ramazani, A., & Taghavi Fardood, S. (2020). Synthesis of Al2O3/ZrO2 nanocomposite and the study of its effects on photocatalytic degradation of reactive blue 222 and reactive yellow 145 dyes. *ChemistrySelect* , 5, 9966–9973.

Zarei, M. (2020). Ultrasonic-assisted preparation of ZrO2/g-C3N4 nanocomposites with high visible-light photocatalytic activity for degradation of 4-chlorophenol in water. *Water-Energy Nexus* , 3, 135–142.

Zarei, M. (2020). Ultrasonic-assisted preparation of ZrO2/g-C3N4 nanocomposites with high visible-light photocatalytic activity for degradation of 4-chlorophenol in water. *Water-Energy Nexus* , 3, 135–142.

Zeyu Guan, S. Z. (2022). Fe–O–Zr in MOF for effective photo-Fenton Bisphenol A degradation: Boosting mechanism of electronic transmission. *Chemosphere*, 134481.

Zhao, W., Adeel, M., Zhang, P., Zhou, P., Huang, L., Zhao, Y., . . . al, e. (2022). A critical review on surface modified nano-catalysts application for photocatalytic degradation of volatile organic compounds. *Environ. Sci Nano*, 9, 61–80.

Zhao, W., Adeel, M., Zhang, P., Zhou, P., Huang, L., Zhao, Y., . . . al, e. (2022). A critical review on surface modified nano-catalysts application for photocatalytic degradation of volatile organic compounds. *Environ. Sci Nano* , 9, 61–80.

Zhou, H., Yao, P., Gong, T., Xiao, Y., Zhang, Z., Zhao, L., . . . Deng, M. (2019). Effects of ZrO2 crystal structure on the tribological properties of copper metal matrix composites. *Tribol. Int*, 380–391.

Copyright to the author of some rights reserved This work is licensed under aCreative Commons Attribution-ShareAlike 4.0 International License.